Differences in Self-Assembly Features of Thermoresponsive Anionic Triblock Copolymers Synthesized via One-Pot or Two-Pot by ATRP

Vahid Forooqi Motlaq,[1] Leva Momtazi,[1] Kaizheng Zhu,[1] Kenneth D. Knudsen,[2] Bo Nyström[1]

[1]Department of Chemistry, University of Oslo, Blindern, P.O. Box 1033, Blindern, N-0315 Oslo, Norway

[2]Department of Physics, Institute for Energy Technology, P. O. Box 40, N-2027 Kjeller, Norway

ABSTRACT: The self-assembly process in aqueous solutions of the methoxyl-poly(ethylene glycol)-*block*-poly(2-acrylamido-2-methyl-1-propanesulfonic sodium)-*block*-poly(*N*-isopropyl acrylamide) (MPEG-*b*-PAMPS-*b*-PNIPAAM) triblock copolymer, synthesized *via* two different atomic transfer radical polymerization (ATRP) methods, namely "one-pot" (P3-sample) and "two-pot" (P2-sample), was studied by various experimental techniques. The "one-pot" procedure leads to a copolymer (P3) where the PNIPAAM block is contaminated with a minor quantity of AMPS residuals and this sample does not form micelles over the considered temperature region, but unimers and temperature-induced aggregates coexist in the presence of a small amount of salt. The P2 polymer forms micelles and intermicellar structures, but the former moieties disappear at high temperatures, whereas the latter species contract with increasing temperature. Small angle neutron scattering results revealed correlation peaks, both for P3 and P2, and no micelle formation for P3, but a pronounced upturn of the scattered intensity at low wave-vector values at elevated temperatures for the P2 copolymer. The findings from this study, clearly show that the spurious AMPS residuals have a drastic influence on the self-assembly and micelle formation of the triblock copolymer.

KEYWORDS: "one-pot" and "two-pot" by ATRP; charged triblock copolymer; self-assembling process; small angle neutron scattering; dynamic light scattering; zeta-potential

INTRODUCTION The interest in design and production of amphiphilic block copolymers has increased significantly in recent years due to their potential use in drug delivery applications.[1-8] Amphiphilic polymers can self-assemble in aqueous medium to form micelles or vesicles with a hydrophobic core and a hydrophilic shell. The hydrophobic core can encapsulate hydrophobic drugs while the hydrophilic shell stabilizes the micellar structure.[9] Organization into these ordered structures can be explained by mechanisms driven by free energy, including van der Waals, electrostatic, hydrogen bonding, and hydrophobic interactions.[10] The structure of block copolymer associations can change in response to external physical and/or chemical stimuli, such as temperature, pH, ionic strength, and solvent composition in a biological environment, which can control release of encapsulated drug.[11,12]

Poly(*N*-isopropylacrylamide) (PNIPAAM) is one of the most studied thermoresponsive polymers. PNIPAAM exhibits a lower critical solution temperature (LCST) around 32° C, below this temperature PNIPAAM is water soluble and above that a macroscopic phase separation takes places.[13,14] This transition from a hydrophilic to hydrophobic nature upon a temperature rise can be employed for designing drug loading and delivery systems. However, as the LCST is approached the "stickiness" of PNIPAAM containing micelles increases and this may lead to intermicellar aggregation. To address this problem and also to increase the stability of the PNIPAAM based micelles, block copolymers containing the hydrophilic poly(ethylene glycol) (PEG) can be designed especially for biomedical applications.[15] In addition to minimizing agglomeration by a steric repulsion mechanism, PEG chains forming a hydrophilic corona can reduce the nonspecific protein adsorption of different nanocarriers in a biological environment, thus increasing their blood circulation half-time and preventing premature uptake of nanocarriers by macrophages.[16,17]

Block copolymers consisting of charged groups and hydrophobic blocks can also form micelles in an aqueous solution. Such micelles are constituted of a hydrophobic core and an ionic corona[18,19] and the micellization process can be controlled by regulating the ionic strength and/or the pH of the aqueous solution.[20-23] As an example, sodium 2-acrylamido-2-methyl-1-propane sulfonate (AMPS) based copolymers are used as stabilizers of colloidal suspensions in pharmaceuticals, cosmetics, and paint and recently employed in various fields of nanotechnology and drug delivery systems.[18]

It has been shown that the polydispersity of block copolymers has a direct influence on the critical micellar concentration (cmc).[18] Therefore, recently controlled/"living" radical polymerization techniques, namely nitroxide mediated radical polymerization (NMRP), reversible addition fragmentation chain transfer (RAFT), and atom transfer radical polymerization (ATRP) have been proposed as the preferred method for synthesis of low polydispersity homopolymers and block copolymers.[18,24,25] The preparation of a well-defined poly[(ethylene oxide)-block-(sodium2-acrylamido-2-methyl-1-propane sulfonate)] diblock copolymer [P(EO_m-b-$AMPS_n$)], was described in 2006 by the ATRP technique, using methoxy-o-(2-methylbromoisobutyrate)poly(ethylene oxide)s (MeO-P$[EO]_m$-Br^{i}B and CuBr. 2Bpy (Bpy for 2,2'-bipyridyl) as macroinitiator and catalytic complex, respectively.[19]

There are two possible routes to synthesize block copolymers by ATRP, "one-pot" and "two- pot" methods. In the "two- pot" method, the first block is isolated and purified and then used as a macroinitiator, whereas in the "one-pot" method the synthesis proceeds through sequential monomer addition. It has been shown previously that the block copolymerization method can affect the micellization behavior.[18] In view of this knowledge, the aim of this investigation is to closely scrutinize the effect of the polymerization method on self-assembly and micellization of an amphiphilic three block

copolymer. In this work, methoxyl-poly(ethylene glycol)-*block*-poly(2-acrylamido-2-methyl-1-propanesulfonic sodium)-*block*-poly(*N*-isopropyl acrylamide) (MPEG-*b*-PAMPS-*b*-PNIPAAM) triblock copolymer was synthesized *via* "one-pot" or "two-pot" ATRP methods. The impact of the synthetic method on the self-assembly properties of the copolymers synthesized with these two methods was investigated utilizing turbidimetry, zeta potential, dynamic light scattering (DLS), and small angle neutron scattering (SANS). These characterization methods revealed fundamental differences in self-assembling and other physical features between the two synthetic methods, which we believe is useful information concerning the optimization of block copolymer synthesis with respect to specific uses in aqueous environments.

EXPERIMENTAL

Materials

2-Bromoisobutyl bromide and copper(II) chloride were both purchased from Sigma-Aldrich and employed as received. *N*-isopropylacrylamide (NIPAAM, Acros) was recrystallized from a toluene/n-hexane mixture and dried under vacuum prior to use. The charged monomer 2-acrylamido-2-methyl-1-propanesulfonic acid sodium salt, abbreviated as AMPS (50 wt% in H_2O, Aldrich), was purified from the trace inhibitor present in the sample by removing most of the water in the vacuum oven at 60 °C, followed by washing with cold ethanol and finally drying under vacuum. Triethylamine (TEA) was dried over anhydrous magnesium sulfate, filtered, distilled under N_2 atmosphere, and stored over 4 Å molecular sieves. Copper(I) chloride from Aldrich was washed with glacial acetic acid, followed by washing with methanol and diethyl ether and then dried under vacuum and kept under N_2 atmosphere. N,N,N',N'',N''',N''''-(hexamethyl triethylene tetramine) (Me_6TREN) was synthesized according to a previous description in the literature.[26] The

synthesis of the MPEG macroinitiator (MPEG-MI) was performed in accordance with a published procedure by the reaction of monomethoxyl-capped poly(ethylene glycol) ($MPEG_{45}$-OH and the data of M_n = 2000 were provided by the manufacturer) with 2-bromoisobutyryl bromide in the presence of trimethylamine.[27] All water used in this study was purified with a Millipore Mill-Q system and the resistivity was less than 18 M Ω cm.

Synthesis of Block Copolymers

As mentioned above, a triblock copolymer was prepared by utilizing a "one-pot" or a "two-pot" procedure. In the first approach, the copolymer was synthesized via a simple **"one-pot"** (referred here as P3) two steps ATRP method (FIGURE 1, right).[18,28-30] Briefly, the polymerization was performed in a water/DMF (50:50, v/v) mixture at 25 °C; the initiator/catalyst system in the mixture contained a MPEG derivative macroinitiator ($MPEG_{45}$-MI), CuCl, $CuCl_2$, and Me_6TREN (with molar feed ratio [AMPS]/[NIPAAM]/[$MPEG_{45}$-MI]/[CuCl]/[$CuCl_2$]/[Me_6TREN] = 30/30/1/1/0.6/1.6, [AMPS]=1M). In a general procedure, the components AMPS (6.87 g, 30 mmol) and MPEG-macroinitiator (2.15 g, 1 mmol), were dissolved in 28 mL of a water/DMF (13mL/15mL) solvent mixture in a 100 mL Schlenk flask under magnetic stirring. The mixture was degassed by bubbling with argon for at least 1 h, before it was immersed in a water-bath that was kept at about 25 °C. A volume of 2 mL of the freshly prepared Cu(I)-Cu(II)-Me_6TREN water stock solution (prepared by adding degassed water (6.3 mL) to CuCl (4 mmol, 0.396 g), $CuCl_2$ (2.4 mmol, 0.322g) and Me_6TREN (6.4 mmol, 1.76 mL) exposed to vigorous stirring under the influence of argon flow) was withdrawn via a syringe and quickly added to the above mixture and the polymerization reaction was then initiated.

When the AMPS monomer conversion reached approximately 90% (after approximately 30 min) ^{1}H NMR analysis on 0.1 mL solution that was withdrawn from the

reaction mixture indicated that more than 90% of the AMPS had been polymerized (disappearance of the vinyl signals at δ = 5.5– 6.0 ppm)). A well degassed solution of NIPAAM (30 mmol, 3.5 g) in a 15 mL water/DMF (50/50, v/v) mixture was then added quickly ([NIPAAM]/[MPEG-MI] = 30/1) to the reaction mixture via a syringe under an atmosphere of argon. After 1 h, the polymerization was stopped by exposing the reaction mixture to air and it was diluted with distilled water. To remove other impurities such as the unreacted monomers, low molecular weight product, organic solvent (DMF), and trace amounts of Cu ions, the resulting mixture was further purified by diluting it with water and it was dialyzed first in the presence of 0.1N NaCl and then against distilled water for 3 weeks, using a dialysis membrane of regenerated cellulose with a molecular weight cut-off of 3500. The white solid product was finally isolated by lyophilization (6.2 g).

In the alternative approach, the triblock copolymer was also synthesized via a "**two-pot**" (referred here as P2) atom transfer radical polymerization procedure (FIGURE 1, left), i.e., the diblock copolymer MPEG-*b*-PAMPS was synthesized, purified, and further employed as the macroinitiator to initiate the polymerization of the second monomer (NIPAAM). The first initiator/catalyst system contained a MPEG macroinitiator ($MPEG_{45}$-MI), CuCl, $CuCl_2$ and Me_6TREN (with molar feed ratio ([AMPS]=1M, [AMPS]/[$MPEG_{45}$-MI]/[CuCl]/[$CuCl_2$]/[Me_6TREN] = 60/1/1/0.6/1.6). The components AMPS (13.74 g, 60 mmol) and MPEG-macroinitiator (2.15 g, 1 mmol), were dissolved in 58 mL of a water/DMF (28mL/30mL) solvent mixture in a 100 mL Schlenk flask under magnetic stirring. A volume of 2 mL of the freshly prepared Cu(I)-Cu(II)-Me_6TREN water stock solution (prepared by adding degassed water (6.3 mL) to CuCl (4 mmol, 0.396 g), $CuCl_2$ (2.4 mmol, 0.322g) and Me_6TREN (6.4 mmol, 1.76 mL) exposed to vigorous stirring under the influence of argon flow) was withdrawn with a syringe and quickly added to the above mixture; the polymerization reaction was then initiated. After 30 min,

the mixture was diluted with water and bubbled with air for 5 min to stop the polymerization. The resulting mixture was further purified by diluting with water, dialyzed first in the presence of 0.1N NaCl and then against distilled water for 2 weeks using a dialysis membrane of regenerated cellulose with a molecular weight cut-off of 3500. A light blue solid product was finally isolated by lyophilization (14.2 g). A MPEG-*b*-P(AMPS)$_m$ sample with m = 56 (P1) was then prepared and subsequently used as the macroinitiator to initiate the polymerization of the second monomer of NIPAAM. The lyophilized MPEG$_{45}$-*b*-P(AMPS)$_{56}$ macroinitiator was dissolved in DMF/water 50/50 (v/v) mixture. The NIPAAM polymerization was then carried out in a similar way as described for the "one-pot" procedure (with molar feed ratio [NIPAAM]/[MPEG$_{45}$-b-P(AMPS)$_{56}$-MI]/[CuCl]/[Me$_6$TREN] = 30/1/1/1, [NIPAAM]=1M). At the end of the polymerization, the mixture was purified by diluting with water, dialyzed first against 0.1N NaCl and then with distilled water. The solid product was finally collected by lyophilization.

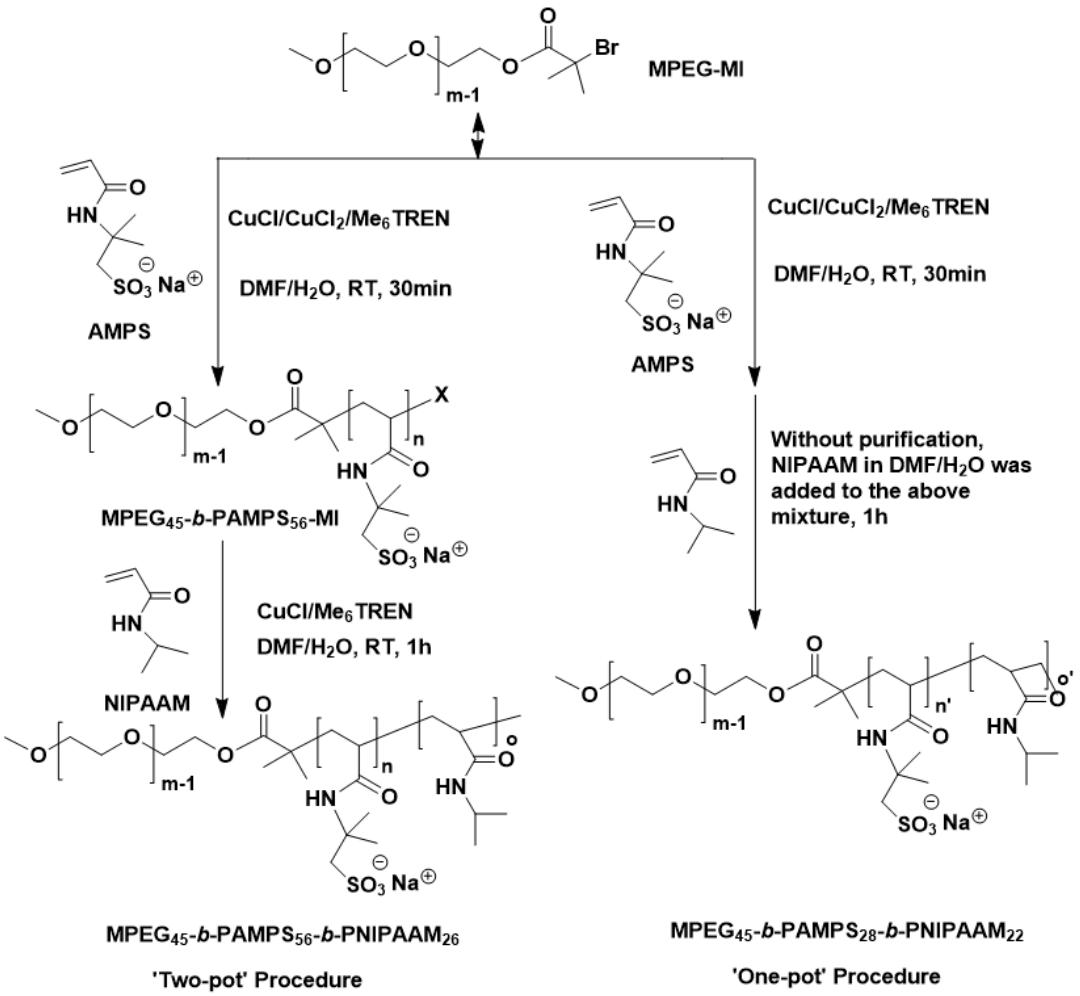

FIGURE 1 Schemes of the synthesis employed for the preparation of MPEG-*b*-PAMPS-*b*-PNIPAAM triblock copolymers *via* ATRP by using "one-pot" or "two-pot" procedure.

The chemical structure of the diblock polymer macroinitiator (MI) and the corresponding triblock copolymers ("one-pot" or "two-pot" procedure) and the approximate length of the three blocks were ascertained by their ^{1}H NMR spectra (FIGURE 2). The ^{1}H chemical shift in D_2O is referred to the residual HDO proton (δ = 4.70 ppm) in D_2O. The values of the *m*, *n*, and *o* in $MPEG_m$-*b*-$PAMPS_n$-MI and $MPEG_m$-*b*-$PAMPS_n$-*b*-$PNIPAAM_o$ were evaluated by comparing the typical peak of the integral area of the methenyl proton of EG (**2**) of MPEG (δ = 3.70 ppm, −OC***H***$_2$C***H***$_2$O-, I_a), the methenyl proton of AMPS (**6**) (δ = 3.30 ppm, −C***H***$_2$SO$_3$, I_b) and the characteristic peak of

NIPAAM (**9**) (δ = 3.82 ppm, −C***H***$(CH_3)_2$, I_c) based on a simple equation: $n_{(AMPS)}$ = 90(I_b/I_a); $o_{(NIPAAM)}$ = 180(I_c/I_a). The composition of the diblock copolymer macroinitiator and triblock copolymers are estimated to be *m/n = 45/56, m/n/o* = 45/56/26 and *m/n'/o'* = 45/28/22, *i.e.,* $MPEG_{45}$-*b*-$PAMPS_{56}$ for P1, $MPEG_{45}$-*b*-$PAMPS_{56}$-*b*-$PNIPAAM_{26}$ for P2 ("two-pot") and $MPEG_{45}$-*b*-$PAMPS_{28}$-*b*-$PNIPAAM_{22}$ for P3 ("one-pot"). We notice that the length of the PAMPS block in P2 is double the length in P3; this should lead to a better electrostatic stabilization of P2 than P3. However, in spite of this the results from this work show that the residual AMPS-charges infecting the PNIPAAM-block in the chain of P3 are more efficient in the stabilization of the unimers than the longer PAMPS spacer in P2. To emphasize the effect of residual charges, we decided to have a much longer PAMPS block in P2.

Information about molecular weights and molecular weight distributions for the samples P1, P2, and P3 were determined in dilute aqueous solutions by means of asymmetric flow field-flow fractionation (AFFFF), and the results are depicted in FIGURE 3.[28] The results show that the samples have low molecular weights and they have narrow molecular weight distributions.

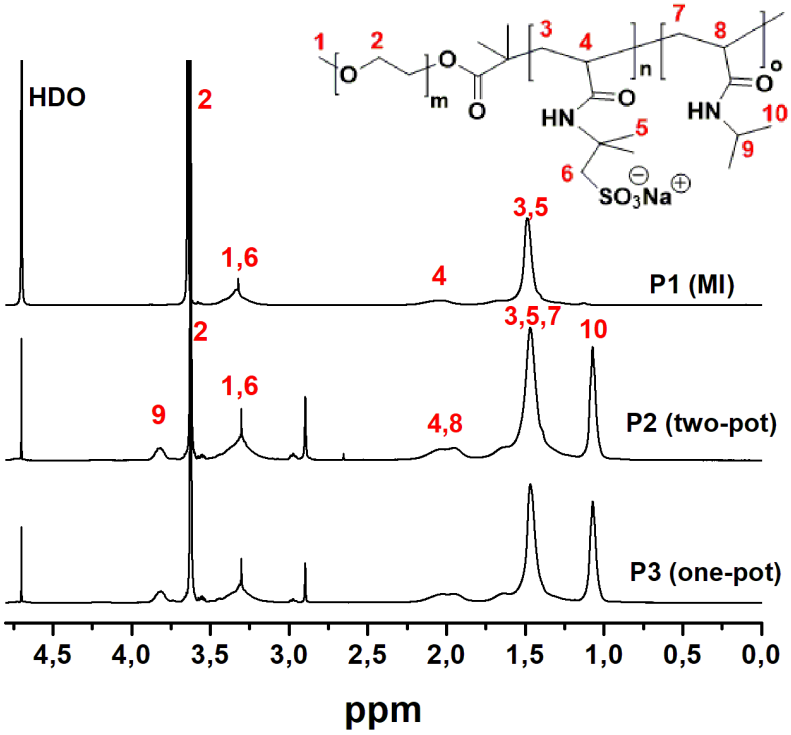

FIGURE 2 ^{1}H NMR spectra of the synthesized copolymers (400 MHz, D_2O): **P1** ($MPEG_{45}$-*b*-$PAMPS_{56}$-macroinitiator); **P2** ($MPEG_{45}$-*b*-$PAMPS_{56}$-*b*-$PNIPAAM_{26}$, "two-pot"); **P3** ($MPEG_{45}$-*b*-$PAMPS_{28}$-*b*-$PNIPAAM_{22}$, "one-pot").

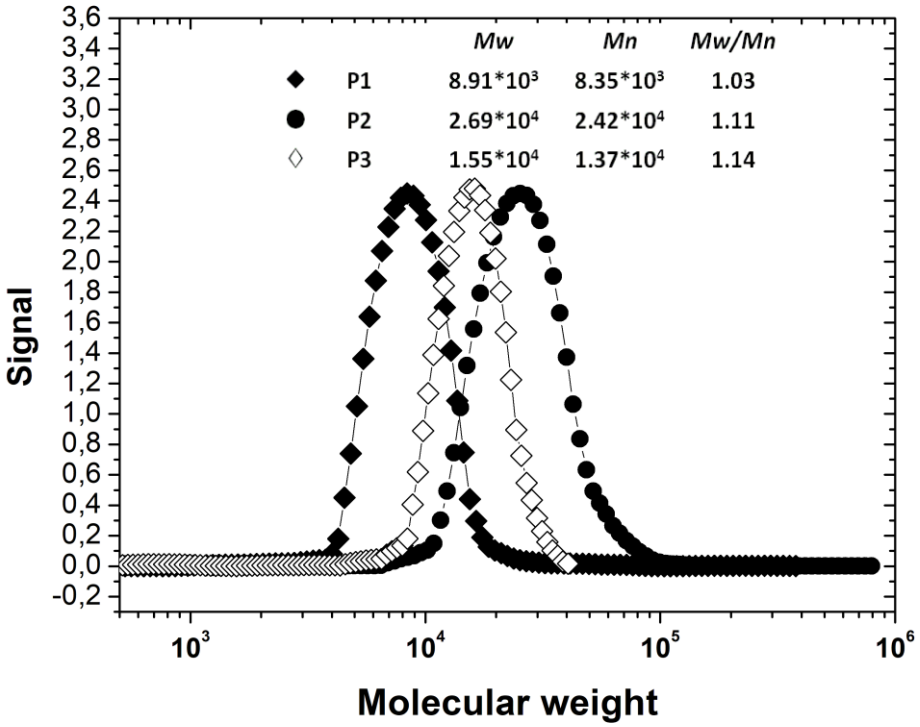

FIGURE 3 Illustration of the molecular weight distribution of the synthesized copolymers in dilute aqueous solution (0.01 N NaCl) with the aid of AFFFF: **P1** ($MPEG_{45}$-*b*-$PAMPS_{56}$-macroinitiator); **P2** ($MPEG_{45}$-*b*-$PAMPS_{56}$-*b*-$PNIPAAM_{26}$, 'two-pot'); **P3** ($MPEG_{45}$-*b*-$PAMPS_{28}$-*b*-$PNIPAAM_{22}$, 'one-pot').

Turbidimetry

Turbidity measurements were performed with a temperature controlled NK60-CPA cloud point analyzer (Phase Technology, Richmond, B.C., Canada). The turbidity of the samples was measured as signal intensity in a temperature range of 10-55 °C. The source of light was an AlGaAs laser with a wavelength of 654 nm. The instrument was provided with a glass plate coated with a thin metallic layer of very high reflectivity, which works as a mirror. The temperature was controlled by a platinum resistance thermometer, providing a temperature range of -60 to +60 °C. For this study the heating rate was set to 0.5°C/min.

Zeta Potential

The zeta potential experiments were conducted on a Malvern Zetasizer Nano ZS (Malvern Instrument Ltd., Worcestershire, UK). The sample cell used was a dip-cell that included palladium electrodes with 2 mm spacing, one 10 mm PMMA cuvette, and a cap. The experiments were carried out at three different temperatures (25, 35, and 45 °C). The instrument determines the electrophoretic mobility of the sample via Laser Doppler Velocimetry (LDV). The following equation for the relationship between electrophoretic mobility (U_E) and ζ potential was applied, $U_E = 2\varepsilon\zeta f(Ka)/3\eta$, where the viscosity (η) and dielectric constant (ε) of water were used. The Smoluchowski approximation to Henry's function (f(Ka) = 1.5) was utilized. The measurements were done in triplicate, and the average value from these runs is reported.

Dynamic Light Scattering

Dynamic light scattering (DLS) experiments were performed using an ALV/CGS-8F multi-detector version compact goniometer system, with 8 fiber-optical detection units, from ALV-GmbH., Langen, Germany. The beam from a Uniphase cylindrical 22mW HeNe-laser was focused on the sample cell (10-mm NMR tubes, Wilmad Glass Co., of highest quality). The laser operates at a wavelength of 632.8 nm with vertically polarized light. The beam passes through a temperature-controlled cylindrical quartz container (with 2 plane-parallel windows) vat (the temperature constancy being controlled to within ±0.01 °C with a heating/cooling circulator), which is filled with a refractive index matching liquid (*cis*-decalin).To avoid dust contamination, the sample solutions were filtered in an atmosphere of filtered air through a 0.8 μm filter (Millipore) directly into pre-cleaned NMR tubes. The DLS experiments were performed at temperatures in the range 25–40 °C and at a polymer concentration of 1 wt%.

For the systems in this work, the scattered field can be assumed to exhibit Gaussian statistics and the experimentally recorded normalized intensity autocorrelation function $g^2(q,t)$ is directly linked to the theoretically amenable first-order electric field autocorrelation $g^1(q,t)$ through the Siegert[31] relationship $g^2(q,t) = 1 + B|g^1(q,t)|^2$,where B ($\leq$1) is an instrumental parameter. The wave vector is defined as $q = (4 \pi n/\lambda) \sin(\theta/2)$, where n is the refractive index of the medium, θ is the scattering angle, and λ is the wavelength of the incident light in a vacuum.

At temperatures up to approximately CP, the correlation functions can be described accurately by the sum of two stretched exponential functions of the Kohlrausch-Williams-Watts type[32,33] as follows

$$g^1(t) = A_f \exp[-(t/\tau_{fe})^{\beta}] + A_s \exp[-(t/\tau_{se})^{\gamma}] \quad (1)$$

with $A_f + A_s = 1$. The parameters A_f and A_s are the amplitudes for the fast and the slow relaxation mode, respectively. The stretched exponents β and γ characterize the widths of the distribution of relaxation times for the fast and the slow mode, respectively. The variables τ_{fe} and τ_{se} are the relaxation times characterizing the fast and the slow relaxation process, respectively. At higher temperatures for the P2 copolymer, when most of the micelles have been consumed in the formation of intermicellar structures and the fraction of large species dominates, the correlation functions could be fitted with a single stretched exponential ($g^1(t) = \exp[-(t/\tau_{se})^{\beta}]$). For the P3 sample, there is a coexistence of unimers and large aggregates over the whole temperature interval and eq 1 is valid.

Bimodal relaxation processes have recently been reported[34-36] from DLS studies on associating polymer systems of various natures. In the analysis of the correlation functions with the aid of eq 1, a nonlinear fitting algorithm was employed to obtain best-fit values of the variables A_f, τ_{fe}, τ_{se}, β, and γ appearing on the right-hand side of eq 1. The

fast relaxation time yields the mutual diffusion coefficient D_f ($\tau_f^{-1}=D_f q^2$) of unimers or micelles, whereas the slow relaxation time produces the mutual diffusion coefficient D_s of large clusters or intermicellar structures. Through the stretched exponents β ($0 < \beta \leq 1$) and γ ($0 < \gamma \leq 1$) the mean relaxation times for the fast and slow mode, respectively, are given by

$$\tau_f = \frac{\tau_{fe}}{\beta}\Gamma\left(\frac{1}{\beta}\right) \quad (1a)$$

$$\tau_s = \frac{\tau_{se}}{\gamma}\Gamma\left(\frac{1}{\gamma}\right) \quad (1b)$$

where Γ is the gamma function. From the relaxation modes, we are able to determine the apparent hydrodynamic radii ($R_{h,f}$ and $R_{h,s}$) from the fast and slow relaxation times, respectively, via the Stokes-Einstein relation $R_h = k_B T/6\pi\eta_0 D$, where k_B is the Boltzmann constant, T is the temperature, η_0 is the solvent viscosity, and D is the mutual diffusion coefficient of unimers or micelles/association complexes. We should note that the Stokes-Einstein relation is strictly valid only in the absence of interparticle interactions and internal motions, that is, $qR_h < 1$. For some very large species considered in this study, this criterion is not fulfilled and some corrections to R_h should be made to obtain accurate values of R_h. However, since we are more concerned with the characteristic growth of clusters with increasing temperature, rather than the real cluster size itself, this correction is not crucial.

Small Angle Neutron Scattering

The SANS measurements were carried out at selected temperatures in the range 10–50 °C with the SANS installation at the JEEP II reactor at IFE, Kjeller. The wavelength was set with the aid of a selector (Dornier), using a wavelength resolution $\Delta\lambda/\lambda$= 10%. The neutron

detector was a 128×128 pixel, He-3 filled RISØ-type, mounted on rails inside an evacuated detector chamber. Two different detector distances of 1.0 to 3.4 m and two wavelengths of 5.1 Å and 10.2 Å were employed to obtain a broad wave-vector range from 0.006 to 0.32 $Å^{-1}$. Here q, the absolute value of the wave-vector, is given by $q=(4\pi/\lambda)\sin(\theta/2)$, where θ is the scattering angle and λ is the neutron wavelength. The samples were held in 2 mm quartz cuvettes, equipped with stoppers. The measuring cells were placed onto a copper base for good thermal contact and mounted in the sample chamber. At each temperature, the samples were allowed to equilibrate before the measurement.

The transmission was measured separately, and the absolute scattering cross section (cm^{-1}) was calculated by taking into account the contribution from empty cell and general background. The samples were prepared in heavy water instead of light water to enhance contrast and reduce incoherent background.

RESULTS AND DISCUSSION

In this work, we have synthesized two MPEG-*b*-PAMPS-*b*-PNIPAAM ionic amphiphilic block copolymers without protecting group chemistry/post-polymerization derivation *via* an aqueous ATRP by using two different procedures (so-called "one-pot" and "two-pot" polymerization). The sequential polymerization of AMPS and NIPAAM without isolation of the first block ("one-pot" polymerization) generates the simplest procedure for the synthesis of the block copolymers without the need for isolation and purification of the first block macroinitiator (MPEG-*b*-PAMPS-MI). In contrast, the "two-pot" procedure encompasses the isolation and purification of the first block macroinitiator (MPEG-*b*-PAMPS-MI) and this method is more time-consuming. The most significant difference between the two procedures is that in the "one-pot" (P3) method a small amount of AMPS (5 mol % with respect to PEG) was still present at the beginning of the NIPAAM

polymerization, whereas no AMPS was present in the "two-pot" (P2) procedure. This leads to a situation where $MPEG_{45}$-*b*-$PAMPS_{56}$-*b*-$PNIPAAM_{26}$ ("two-pot") contains a pure PNIPAAM block, whereas $MPEG_{45}$-*b*-$PAMPS_{28}$-*b*-$PNIPAAM_{22}$ ("one-pot") contains a PNIPAAM block with an average of 1-2 AMPS residues per copolymer chain. Even though the "one-pot" procedure *via* the sequential monomer addition would be an easier way to prepare this type of block copolymers, the small amount of the residual AMPS monomer present during the initial stage of the NIPAAM polymerization, may have an impact on the micellization process and other characteristic physical properties of the copolymer. A schematic illustration of the influence is depicted in Figure 4.

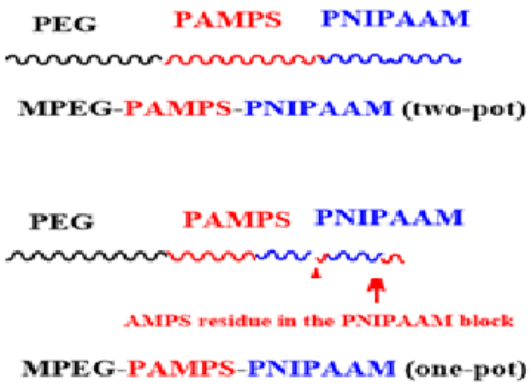

FIGURE 4 A simplified schematic illustration of synthesis defects in the "one-pot" compared with the "two-pot" procedure.

Turbidity and Zeta Potential

Turbidity measurements were conducted on aqueous solutions of P2 and P3 to monitor temperature-induced thermodynamic alterations and aggregation. Samples were prepared in pure D_2O, as well as with addition of 0.01 M NaCl. In solutions of P2, a pronounced upturn of the turbidity is observed at approximately 35 ^{o}C and the effects of salinity and

polymer concentration on the sharp transition are modest (see Figure 5a). The strong upturn of the turbidity indicates formation of aggregates and intermicellar structures; this is mainly attributed to the enhanced sticking probability of the PNIPAAM blocks as the temperature rises and thereby large association complexes are formed. This type of feature has previously been reported for charged PNIPAAM-based block copolymers.[21,28,29,37] In the case of P3 a quite different scenario evolves, where virtually no change of the turbidity is detected in the considered temperature domain for the two polymer solutions without added salt, whereas for the solution with added salt a prominent upturn of the turbidity is found at about 50 ^{o}C (see Figure 5b). This latter behavior can probably be ascribed to screening of the electrostatic interactions and thereby promoting stickiness and development of intermicellar structures.

The prominent difference in turbidity behavior between the solutions of P2 and P3 is astonishing, because while the NIPAAM block length is approximately the same for both copolymers, the AMPS block length in P2 is twice that of P3. This is a hydrophilic and charged block that is anticipated to stabilize the micelles electrostatically; in view of this it is expected that the P2 copolymer with a much longer AMPS block should need considerably higher temperature than P3 to self-assemble and form intermicellar complexes, but the opposite is true. This unexpected behavior can probably be rationalized in the following way. By using the "one-pot" ATRP procedure, it is anticipated that the PNIPAAM-blocks will be adulterated with AMPS entities and this will diminish the sticking power of the PNPAAM-blocks at elevated temperatures and thereby postpone the formation of intermicellar complexes to higher temperatures.

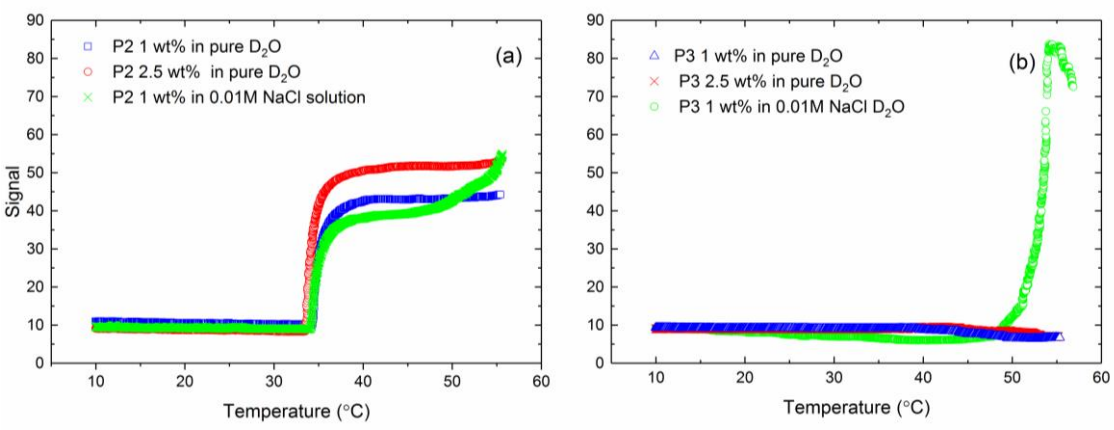

FIGURE 5 Effects of temperature, polymer concentration, and salinity on the turbidity for solutions of the copolymers P2 (two-pot) (a) and P3 (one-pot) (b).

The zeta potential yields information about the charge density on the surface of micelles or intermicellar complexes and may be an indicator of stability and structure of the species. The effect of temperature on the zeta potential for P2 and P3 is illustrated in Figure 6. At 25 ^{o}C the value of the zeta potential is almost the same (-25 mV due the sulfite groups in the AMPS block) for the two copolymers, which supports our hypothesis that the PNIPAAM-blocks are infested by AMPS entities, since P2 should have a higher charge density than P3 due to the much longer PAMPS-block . In the case of P2, it is evident that the charge density increases strongly with rising temperature. This can probably be ascribed to contraction of the association complexes when the NIPAAM segments in the core of the structure are close-packed. As a consequence charges are pressed out onto the surface as the temperature rises. The fact that the turbidity levels off at temperatures above 40 ^{o}C (cf. Figure 5a) may portend electrostatic stabilization of the species. In the presence of salt, there is still an increase of the turbidity at high temperatures. A similar temperature-induced charge density increase has recently been reported[37,38] for aqueous solutions of various charged amphiphilic copolymers.

In the case of P3, the zeta potential is virtually not affected by temperature in the considered temperature region. Our conjecture is that the insertion of AMPS segments in the PNIPAAM-block prevents the unimers to self-assemble into micelles and intermicellar structures. This idea is further reinforced by the DLS and SANS results reported below. In the presence of only unimers, a major compression of these entities and a considerable alteration of the zeta potential are not foreseen.

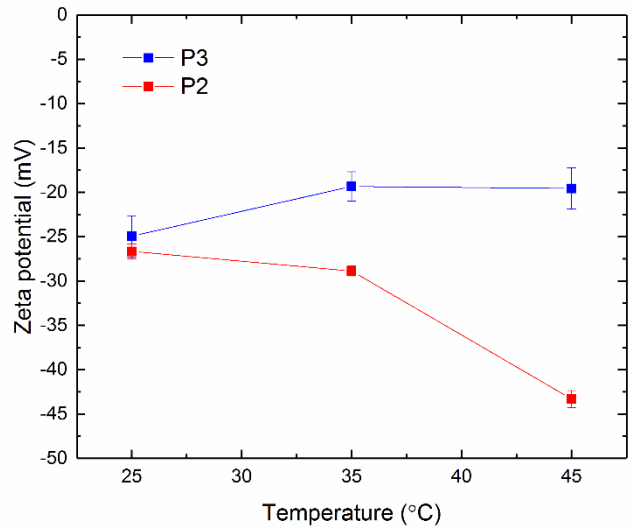

FIGURE 4 Temperature dependence of the zeta potential in aqueous solutions (1 wt%) of the copolymers P2 and P3.

Dynamic Light Scattering

In this study DLS was used to monitor the micellization behavior of P2 and P3 solutions by measuring the hydrodynamic radius and size distribution of the samples in the temperature range of 20-60 °C.

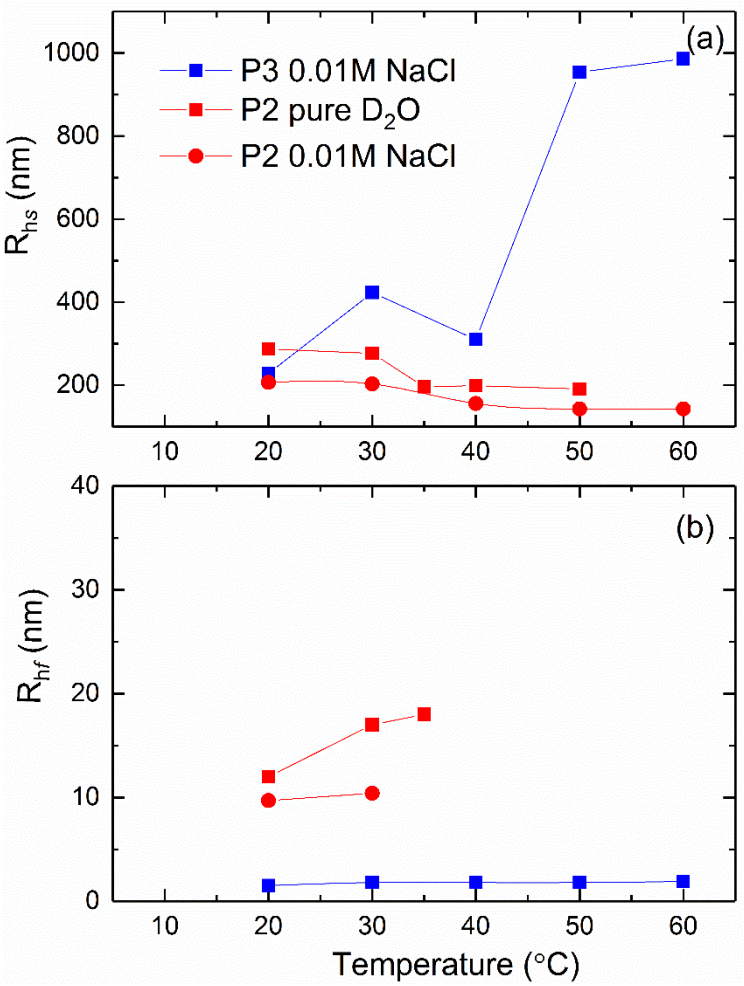

FIGURE 5 Temperature dependencies of the apparent hydrodynamic radii determined from the slow relaxation time ($R_{h,s}$) (a) and the fast relaxation time ($R_{h,f}$) (b) through the Stokes–Einstein relationship for the systems indicated.

For P2 solutions in pure D_2O and with added NaCl, well-defined correlation functions were observed at all conditions; the relaxation process was bimodal with coexistence of micelles and intermicellar aggregates ($R_{h,f} \leq$ 18 nm, $R_{h,s} \leq$ 287 nm at 30 ^{o}C) up to 35 ^{o}C in absence of salt and up to 30 ^{o}C ($R_{h,f} \leq$ 10nm, $R_{h,s} \leq$ 207 nm) in the presence of salt (see Figure 7). Interestingly, micelles are formed already at 20 ^{o}C, well below the cloud point (ca. 33 ^{o}C, Figure 5). The same behavior has been reported for other PNIPAAM-based

copolymers.[39] At higher temperatures, both with and without salt, larger species in the system grow at the expense of the smaller ones in the spirit of Ostwald ripening[37,40] . The correlation functions become unimodal and can be well-described by a single stretched exponential with values of β approaching 1, suggesting a collection of species with narrow size distribution at high temperatures. This may be related to the high charge density observed for these moieties at high temperatures. This feature has been reported and discussed previously for uncharged and charged amphiphilic copolymers[37.41] and quite recently an interesting review on this phenomenon was presented.[42] The results for 1 wt% solutions of P2, both with and without salt, show a compression of the intermicellar complexes ($R_{h,s}$) as the temperature rises (Figure 7a). This compaction of the species can probably be attributed to dehydration of the PNIPAAM segments and closer packing of the segments because of augmented hydrophobic interactions. The micelles of P2 ($R_{h,f}$, Figure 7b) are nearly of the same size (ca. 10 nm) at 20 ^{o}C, both in the absence and presence of added salt, but in the solution without salt a slight expansion is observed with increasing temperature prior to the disappearance of the micelles into the association complexes. This may indicate that some larger units contribute to the fast relaxation mode.

For the solutions of P3 (1 wt%) in the absence of salt addition, the scattered intensity was very low over the considered temperature domain (20-60 ^{o}C); the correlation functions were dominated by noise and it was not possible to properly fit the correlation functions to extract relaxation times. The reason for this problem can be rationalized in the following way. Under these conditions, the P3 solution consists only of molecularly dispersed small unimers and the density fluctuations from these entities are too low to build-up a correlation function. In the case of P2, micelles and intermicellar structures were formed at low temperatures and these bigger species gave rise to apt correlation functions. Our hypothesis is that the insertion of AMPS groups into the PNIPAAM blocks

for the P3 copolymer generates electrostatic stabilization of the unimers, even at elevated temperatures, so that they resist the self-assembly process to form copolymer micelles, contrary to the case of P2, where the charges are only located in the PAMPS-spacer block.

However, when salt is added to solutions of P3 a quite different scenario emerges. In this case, the relaxation process is bimodal and a situation evolves where unimers ($R_{h,f} \leq$ 2 nm) coexist with larger association complexes over the whole temperature range (20-60 °C) (see Figure 7). By adding salt to a solution with a charged copolymer there are in principle two effects that come into play, namely screening of electrostatic interactions and the Hofmeister effect.[43] The latter one is sensitive to high ionic strength in polymer solutions, and the presence of the Cl^- anion - due to its location in the Hofmeister series[43,44] frequently leads to higher surface tension, lower solubility of the macromolecules, and salting-out phenomena (aggregation of molecules). It is well-known that salt-addition to solutions of PNIPAAM-based polymers leads to a lower cloud point[45,46] and stronger association effect, but in the present work the salt concentration is much lower (0.01 M) than in the cited studies (0.1-1 M) so it is unlikely that the Hofmeister effect should come into play in the present investigation. The DLS results for P3 in the presence of 0.01M NaCl indicate that we over the entire temperature interval have a situation where unimers coexist with gradually larger aggregates as the temperature increases. This means that from the start we have a reservoir with unimers, and at 20 ^oC the unimers coexist with aggregates (ca. 200 nm) of practically the same size as the intermicellar species from P2, but as the P2 species are stabilized and shrink with increasing temperature the P3 aggregates continue to grow as the temperature rises and assume a size of approximately 1000 nm at 60 ^oC. It is obvious that the P3 copolymer in the presence of salt does not self-assemble in a regular way as the P2 copolymer. This can probably be traced to the spurious charge distribution in the P3 polymer.

Small Angle Neutron Scattering

To gain insight into local structural changes, SANS experiments were carried out on 1 and 2.5 wt% of P2 and P3 polymer solutions over an extended temperature range (10-50 °C). For solutions of P3 we note that the scattering is weak (only around 0.1 cm^{-1} in absolute units), indicating that micelles are not formed in this system at the conditions considered (see Figure 8). In spite of the weak scattering, it is possible to determine (see the inset of Figure 8b) the radius of gyration (R_g = 1.5 nm) and this value is close to the value of the hydrodynamic radius of 2 nm found from DLS. An inspection of the SANS-curves reveals a clear sign of a correlation peak at ca. 0.045 $Å^{-1}$ for the 1 wt% sample and at 0.06 $Å^{-1}$ for the 2.5 wt% sample (Figure 8a). This corresponds to an interaction distance of $d=2\pi/0.045$ = 140 Å (or 14 nm) and 105 Å (or 10.5 nm), respectively. This correlation peak is likely due to the Coulomb repulsion between the charged groups (PAMPS). As one would expect, the correlation distance becomes shorter with increased polymer concentration. Note that the peak position is independent of temperature (from 10 to 50 °C); this shows that the charge interaction is clearly the dominating contribution to the total energy of the system. There is only a small, although systematic, increase in the overall intensity with temperature, but the position of the peak is highly stable (at each concentration). It thus seems like the hydrophobic interaction term from PNIPAAM is not able to create dehydration and tight packing in this system, due to the strong opposing force from the charges. This substantiates the problems we had from DLS to determine the correlation functions and size of the entities from this P3 sample.

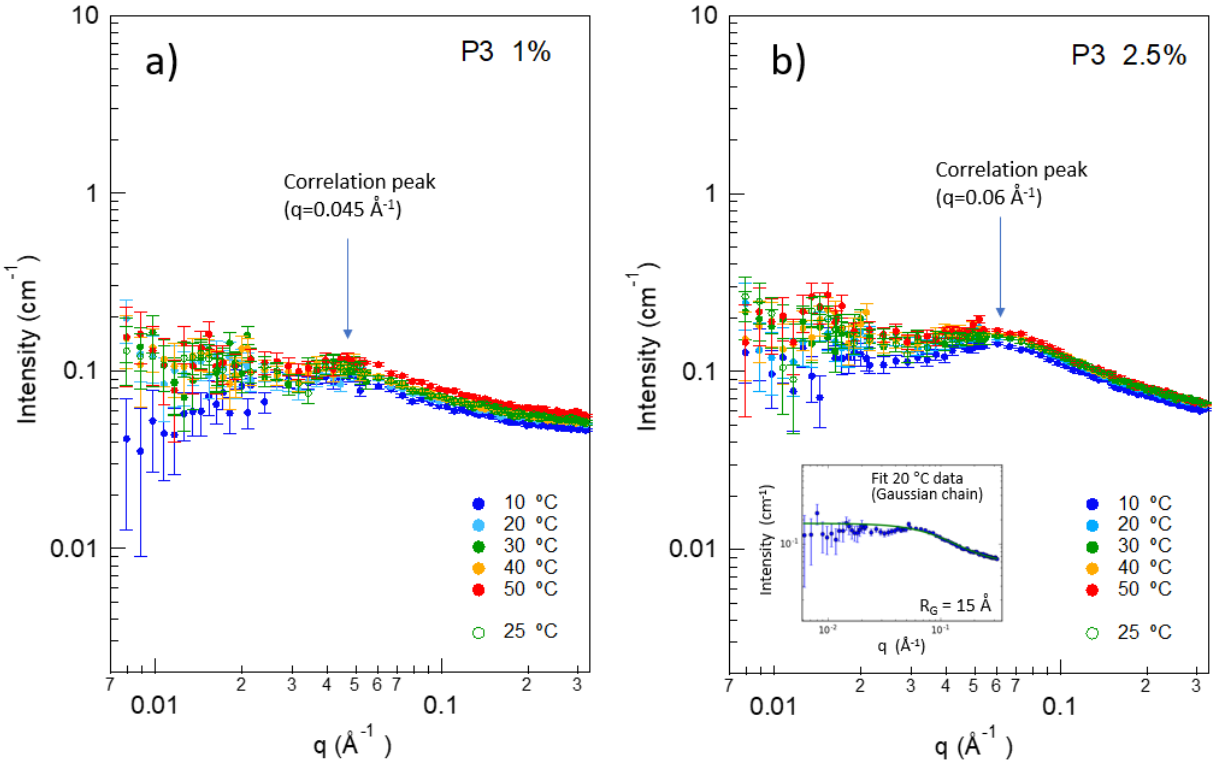

FIGURE 8 SANS patterns of the P3 polymer for the temperatures indicated, and for two different concentrations, a) 1 wt% and b) 2.5 wt%. The inset in b) is a Gaussian coil model fit to the 20 C data at 2.5 wt% concentration.

As the turbidity and DLS results demonstrated, the behavior of P2 and P3 is quite different, especially at elevated temperatures, and this is further emphasized in the SANS results for the P2 sample (see Figure 9). In the q-window accessible for SANS, the SANS results show that up to ca. 30 ^{o}C the two copolymers have common features, with a correlation peak appearing also for P2 at ca. 0.045 Å^{-1} for the 1 wt% sample and at 0.06 Å^{-1} for the 2.5 wt% solution. However, when heated to 40 °C, the low-q intensity increases by a factor of about 100 for P2 (and the increase is even stronger for the 2.5 wt% sample). This indicates the formation of more compact structures in the system, an effect that did not occur with P3. The absence of a plateau in the scattered intensity at low q-values suggests the evolution of large structures (from DLS $R_{h,s}$ is approximately 200 nm, see

Figure 7a) and the size (radius of gyration) of these species cannot be determined in the accessible q-window. However, the slope of -4 is the typical sign of large structures with an average spherical overall shape (Porod scattering).

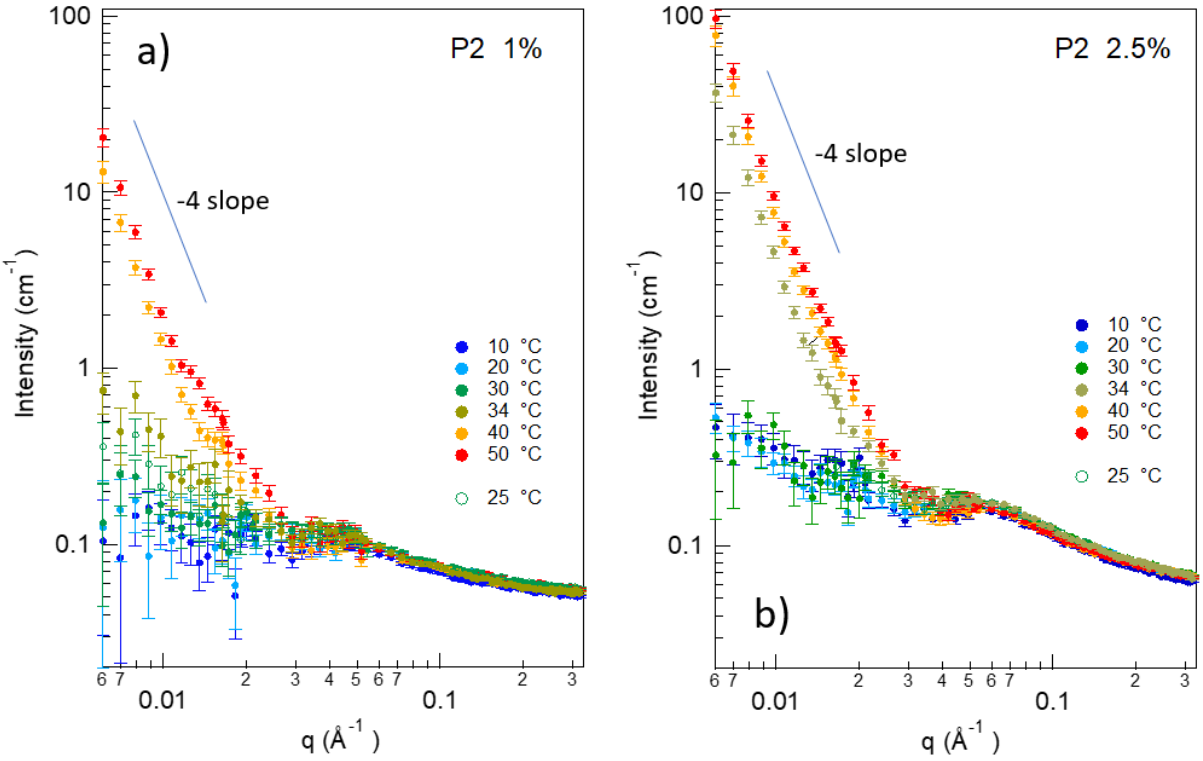

FIGURE 9 SANS patterns of the P2 polymer for the temperatures indicated, and for two different concentrations, a) 1 wt% and b) 2.5 wt%. A line with a slope of -4 (log-log) has been included in both figures to illustrate the Porod-type low-q scattering due to large particles.

As mentioned above, we should bear in mind that a significant difference between the two polymers is the length of the PAMPS block, which is twice as large for P2. This would suggest a better electrostatic stabilization of the P2 polymer, but all the results endorse the opposite to be true. As discussed above, this is attributed to the AMPS residues

present in the NIPAAM block in the P3 solution, which prohibits dehydration and compaction of the hydrophobic block and prevents the micellization process. A close inspection of the SANS patterns (Figure 9) shows that from 40 to 50 ^{o}C little change in the pattern is observed for P2, showing that the packing/dehydration take near full effect between 30 and 40 °C. This finding is consistent with the DLS results (cf. Figure 7a).

Finally, for all samples a measurement was done at 25 °C after the heating cycle (open circles in the plots above). All patterns then returned to the initial values (within the noise level), thus the system is fully temperature-reversible and no hysteresis effects could be found.

These results indicate that a small number of residual charges inserted in the PNIPAAM block are more efficient for the electrostatic stabilization of the polymer than to have a long charged spacer block where all the charges are collected.

CONCLUSIONS

Various experimental methods have been employed to study the self-assembly process in aqueous solutions of the MPEG-*b*-PAMPS-*b*-PNIPAAM triblock copolymer synthesized via two different ATRP synthetic methods, namely “one-pot” (P3-sample) and “two-pot” (P2-sample). The results clearly show fundamental differences in the physical features of the two copolymers. The unimers of the P3 copolymer do not self-assemble to form micelles, not even at elevated temperatures and increased polymer concentration. The SANS measurements disclosed a correlation peak at intermediate q-values and the peak position was found to be independent of temperature and ascribed to electrostatic interactions. Upon addition of a small amount of salt (0.01 M) to the P3-solution, electrostatic interactions are screened and a drastic change of the behavior occurred. In this case a strong increase of the turbidity was observed at higher temperatures, and the DLS

results revealed the coexistence of unimers and gradually larger aggregates as the temperature raised. This is a strong support of a situation where the unimers are electrostatically stabilized in the absence of added salt.

The situation is quite different for the copolymer prepared through the "two-pot" (P2) procedure. In this case the turbidity showed a strong upturn at elevated temperatures, both without and with added salt, and DLS divulged the coexistence of micelles and intermicellar structures. The latter species were found to contract at higher temperatures and the micelles were consumed at sufficiently high temperatures by the intermicellar complexes. The SANS results showed correlation peaks also in this case but a strong upturn of the scattered intensity at low q-values was observed at high temperatures. This signalized the appearance of large aggregates outside the q-window probed by SANS. The self-assembling processes for P3 and P2 are schematically illustrated in Figure 10.

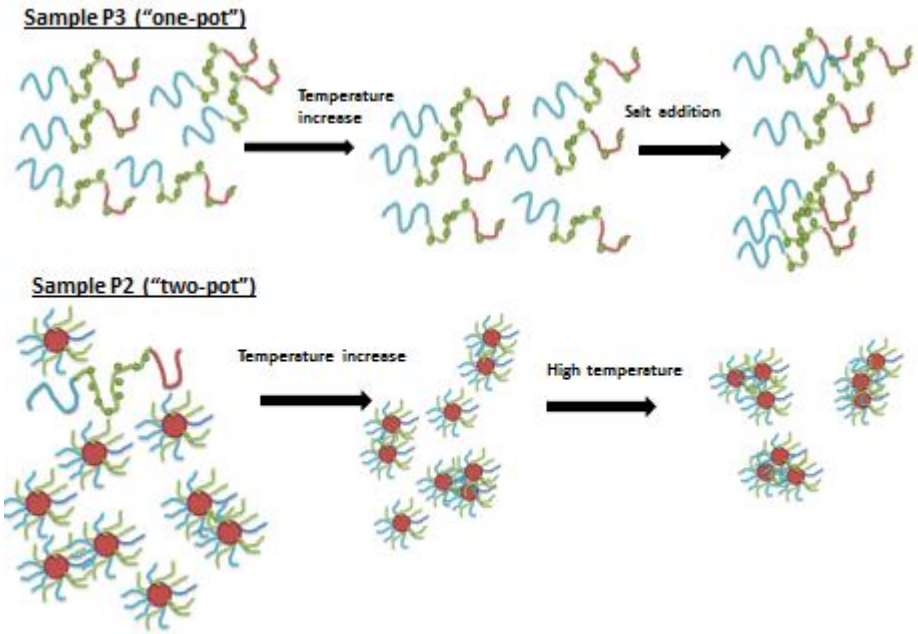

FIGURE 10 A schematic illustration of the self-assembling process for the triblock copolymers (blue-MPEG, green-AMPS-block with charges, and red-PNIPAAM)

synthesized through “one-pot” or “two-pot” ATRP. For P3, unimers are shown at low and high temperatures and aggregates are formed in the presence of added salt. For P2, micelles and intermicellar complexes coexist at low and moderate temperatures, whereas at high temperature micelles are consumed into intermicellar complexes with a narrow size distribution.

Since both copolymers (prepared via “one-pot” or the “two-pot” ATRP synthesis) have approximately the same NIPAAM length we conclude that AMPS residues contaminating the NIPAAM block are responsible for prohibition of the micellization process for the polymer prepared with the “one-pot” method. The findings from this work suggest that the infection of the PNIPAAM block with AMPS residues neutralizes the sticking power of the PNIPAAM block and thereby prevents self-assembly and micellization. This study has demonstrated that the “two-pot” synthesis is a more reliable method for synthesizing this three block copolymer and that a small amount of residual AMPS groups has a crucial impact on the self-assembly of the copolymer in solution.

ACKNOWLEDGMENTS

We sincerely thank Prof. Anna-Lena Kjøniksen for carrying out the AFFFF measurements. B.N greatly appreciates the financial support of the European Union through the NanoS3 project (GrantNo. 290251) of the FP7-PEOPLE-2011-ITN call.

REFERENCES AND NOTES

1 G.S. Kwon, K. Kataoka, *Adv. Drug Delivery Rev.* **1995**, *16* 295.

2 Y. Kakizawa, K. Kataoka, *Adv. Drug Delivery Rev.* **2002**, *54*, 203.

3 A. Agarwal, R. Unfer, S.K. Mallapragada, *J. Control. Release* **2005**, *103*, 245.

4 *Block Copolymers in Nanoscience*; M. Lazzari, G. Liu, S. Lecommandoux, Ed.; Wiley-VCH: Weinheim, Germany, 2006.

5 E.V. Batrakova, A. V. Kabanov, *J. Control. Release* **2008**, *130*, 98.

6 T. Schnitzler, A. Herrmann, *Acc. Chem. Res.* **2012**, *45*, 1419.

7 M.T. Calejo, A.M.S. Cardoso, A.-L. Kjøniksen, K. Zhu, C.M. Morais, S.A. Sande, A.L. Cardoso, M.C.P. de Lima, A. Jurado, B. Nyström, *Int. J. Pharm.* **2013**, *448*, 105.

8 S. Eskandari, T. Guerin, I. Totha, R. J. Stephenson, *Adv. Drug Delivery Rev*. **2017**, **110-111,** 169.

9 G.-K. Xu, X.-Q. Feng, Y. Li, *J. Phys. Chem. B* **2010**, *114*, 1257.

10 N. Gjerde, K. Zhu, B. Nyström, K.D. Knudsen, *Phys. Chem. Chem. Phys.* **2018,** *20* 2585.

11 J. Ko, K. Park, Y.-S. Kim, M. S. Kim, J. K. Han, K. Kim, R.-W. Park, I. S. Kim, H. K. Song, D. S. Lee, I. C. Kwon, *J. Controlled Release* **2007,** *123*, 109.

12 C. He, C. Zhao, X. Chen, Z. Guo, X. Zhuang, X. Jing, *Macromol. Rapid Commun.* **2008,** *29*, 490.

13 H. G. Schild, *Prog. Polym. Sci.* **1992**, *17*, 163.

14 R. Pamies, K. Zhu, A.-L. Kjøniksen, B. Nyström, *Polym. Bull*. **2009**, *62*, 487.

15 V. F. Motlaq, K D. Knudsen, B. Nyström, *J. Colloid Interface Sci.* **2018,** *524*, 245.

16 F. Alexis, E. Pridgen, L. K. Molnar, O. C. Farokhzad, *Molecular Pharmaceutics* **2008,** *5* , 505.

17 Z. Amoozgar, Y. Yeo, *Wiley Interdisciplinary Reviews: Nanomedicine and Nanobiotechnology* **2012,** *4*, 219.

18 G. Masci, D. Bontempo, N. Tiso, M. Diociaiuti, L. Mannina, D. Capitani, V. Crescenzi, *Macromolecules* **2004,** *37,* 4464.

19 D. Paneva, L. Mespouille, N. Manolova, P. Degée, I. Rashkov, P. Dubois, *Macromol. Rapid Commun.* **2006,** *27,* 1489.

20 J. Kötz, S. Kosmella, T. Beitz, *Prog. Polym. Sci.* **2001,** *26,* 1199.

21 A.-L. Kjøniksen, K. Zhu, M. A. Behrens, J. S. Pedersen, B. Nyström**,** *J. Phys. Chem. B* **2011**, *115,* 2125.

22 M. A. Behrens, A.-L. Kjøniksen, K. Zhu, B. Nyström, J. S. Pedersen, *Macromolecules* **2012**, *45,* 246 .

23 M. A. Behrens, M. Lopez, A.-L. Kjøniksen, K. Zhu, B. Nyström, J. S. Pedersen, *Langmuir* **2012**, *28,* 1105.

24 C. J. Hawker, A. W. Bosman, E. Harth, *Chem. Rev.* **2001**, *101,* 3661.

25 Matyjaszewski, K.; Xia, J. *Chem. Rev.* **2001**, *101,* 2921.

26 M. Ciampolini, N. Nardi, *Inorganic Chemistry* **1966,** *5,* 1150.

27 S. Liu, J. V. Weaver, Y. Tang, N. C. Billingham, S. P. Armes, K. Tribe, *Macromolecules* **2002,** *35,* 6121.

28 A.-L. Kjøniksen, K. Zhu, R. Pamies, B. Nyström, *J. Phys. Chem. B* **2008,** *112,* 3294.

29 N. Beheshti, K. Zhu, A.-L. Kjøniksen, K. D..; Knudsen, B. Nyström, *Soft Matter* **2011,** *7,* 1168.

30 Z. Quan, K. Zhu, K. D. Knudsen, B. Nyström, R. Lund, *Soft Matter* **2013,** *9,* 10768.

31 A. Siegert, Radiation Laboratory report no. 465. *Massachusetts Institute of Technology, Cambridge, MA* **1943**.

32 R. Kohlrausch, *Annalen der Physik* **1854,** *167*, 179.

33 G. Williams, D. C. Watts, *Transactions Faraday Society* **1970,** *66*, 80.

34 A.-L. Kjøniksen, B. Nyström, H. Tenhu, *Colloids Surf. A Physicochem. Eng. Aspects* **2003**, *228*, 75.

35 H. Chen, X. Ye, G. Zhang, Q. Zhang, *Polymer* **2006**, *47*, 8367.

36 A. Maleki, A.-L. Kjøniksen, K. Zhu, B. Nyström, *J. Phys. Chem. B* **2011**, *115*, 8975.

37 S. Bayati, K. Zhu, L. T. Trinh, A.-L. Kjøniksen, B. Nyström, *J. Phys. Chem. B* **2012,** *116*, 11386.

38 R. Pamies, K. Zhu, S. Volden, A.-L. Kjøniksen, G. Karlsson, W. R. Glomm, B. Nyström**,** *J. Phys. Chem.* **2010**, *C 114*, 21960.

39 L. Škvarla, J. Zedník, M. Šlouf, S. Pispas, M. Šteˇpánek, *Eur. Polym. J.,* **2014**, *61*, 124.

40 W. Ostwald, *Analytische Chemie*, 3rd ed.; Engelmann: Leipzig, Germany, 1901; p 23.

41 F. Kahnamouei, K. Zhu, R. Lund, K. D. Knudsen, B. Nyström, *RSC Adv.*, **2015**, *5*, 46916.

42 J. R. Shimpi, D. S. Sidhaye, L. V. Prasad, *Langmuir* **2017**, *33*, 9491.

43 F. Hofmeister, Arch Exp Pathol Pharmakol **1888**, *24*, 247.

44 W. Kunz J. Henle B. W. Ninham, *Curr. Opin. Colloid Interface Sci*. **2004**, *9*, 19.

45 Y. Zhang P. S. Cremer, *Curr Opin Chem Biology* **2006**, *10*, 658.

46 S. Fanaian, N. Al-Manasir, K. Zhu, A.-L. Kjøniksen, B. Nyström, *Colloid Polym. Sci.* **2012**, *290*, 1609.

GRAPHICAL ABSTRACT

Vahid Forooqi Motlaq, Leva Momtazi, Kaizheng Zhu, Kenneth D. Knudsen, Bo Nyström

Differences in self-assembly features of thermoresponsive anionic triblock copolymers synthesized via one-pot or two-pot by ATRP

Thermosensitive anionic triblock copolymers of methoxyl-poly(ethylene glycol)-*block*-poly(2-acrylamido-2-methyl-1-propanesulfonic sodium)-*block*-poly(*N*-isopropyl acrylamide) (MPEG-*b*-PAMPS-*b*-PNIPAAM) were synthesized *via* two different atomic transfer radical polymerization (ATRP) methods, namely "one-pot" and "two-pot". The "one-pot" procedure led to a copolymer where the PNIPAAM block is contaminated with a minor quantity of AMPS residuals, whereas no AMPS-contamination of the PNIPAAM block occurred in the "two-pot" procedure. The latter method gave rise to micelles and intermicellar structures in aqueous solution at elevated temperatures, whereas the "one-pot" procedure only produced stabilized unimers at all conditions.